Zbigniew P. Piotrowski

Numerical realization of thermal convection at kilometer scale

Institute of Meteorology and Water Management
– National Research Institute,
Warsaw, Poland

Purpose of this talk

- To relearn the lesson of linear theory, governing the development of atmospheric convection in Greyzone, especially the organized convection.

- To advertise the numerical tools allowing for examination of numerical effects on the convective weather patterns

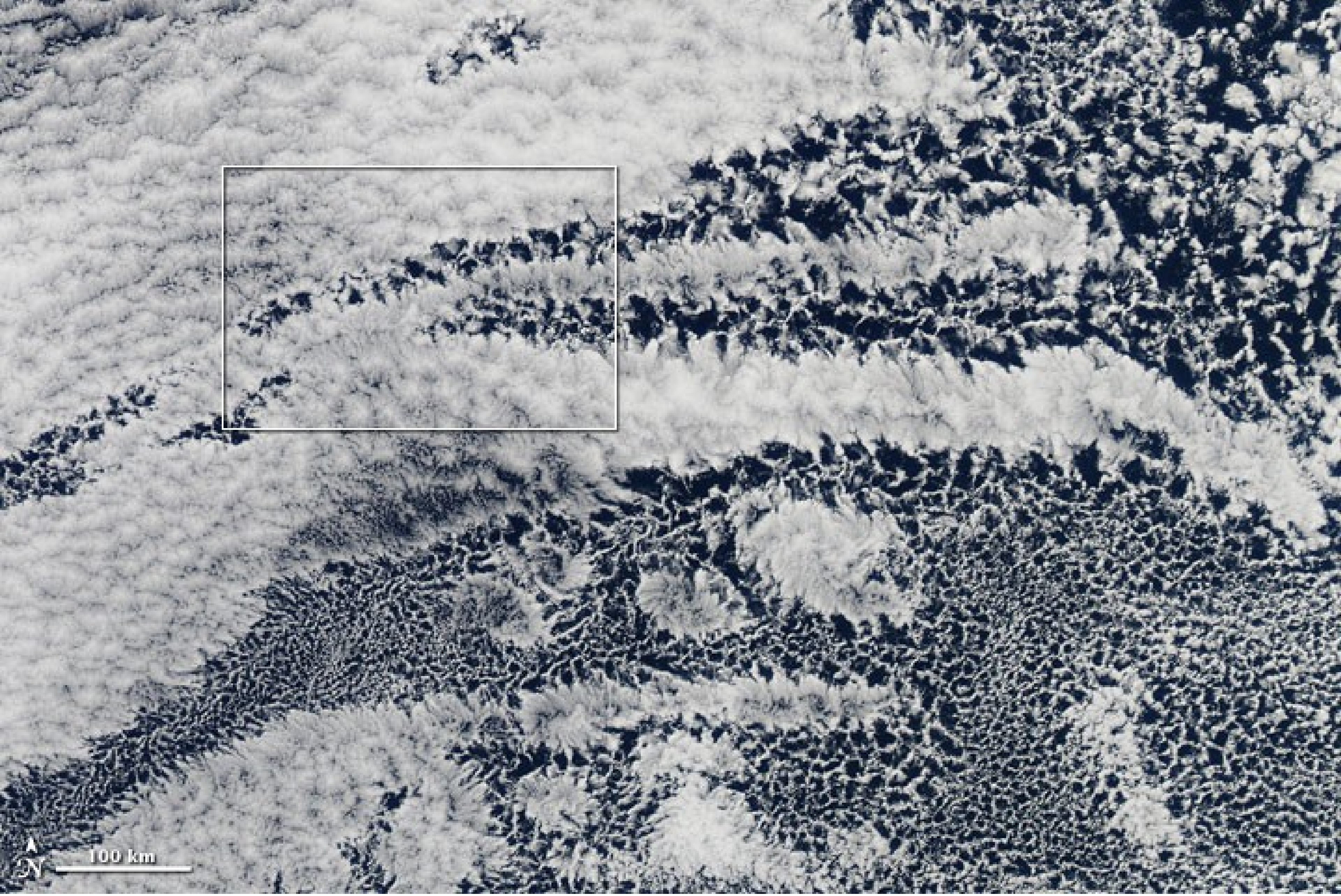

Open and closed cells forming in maritime conditions

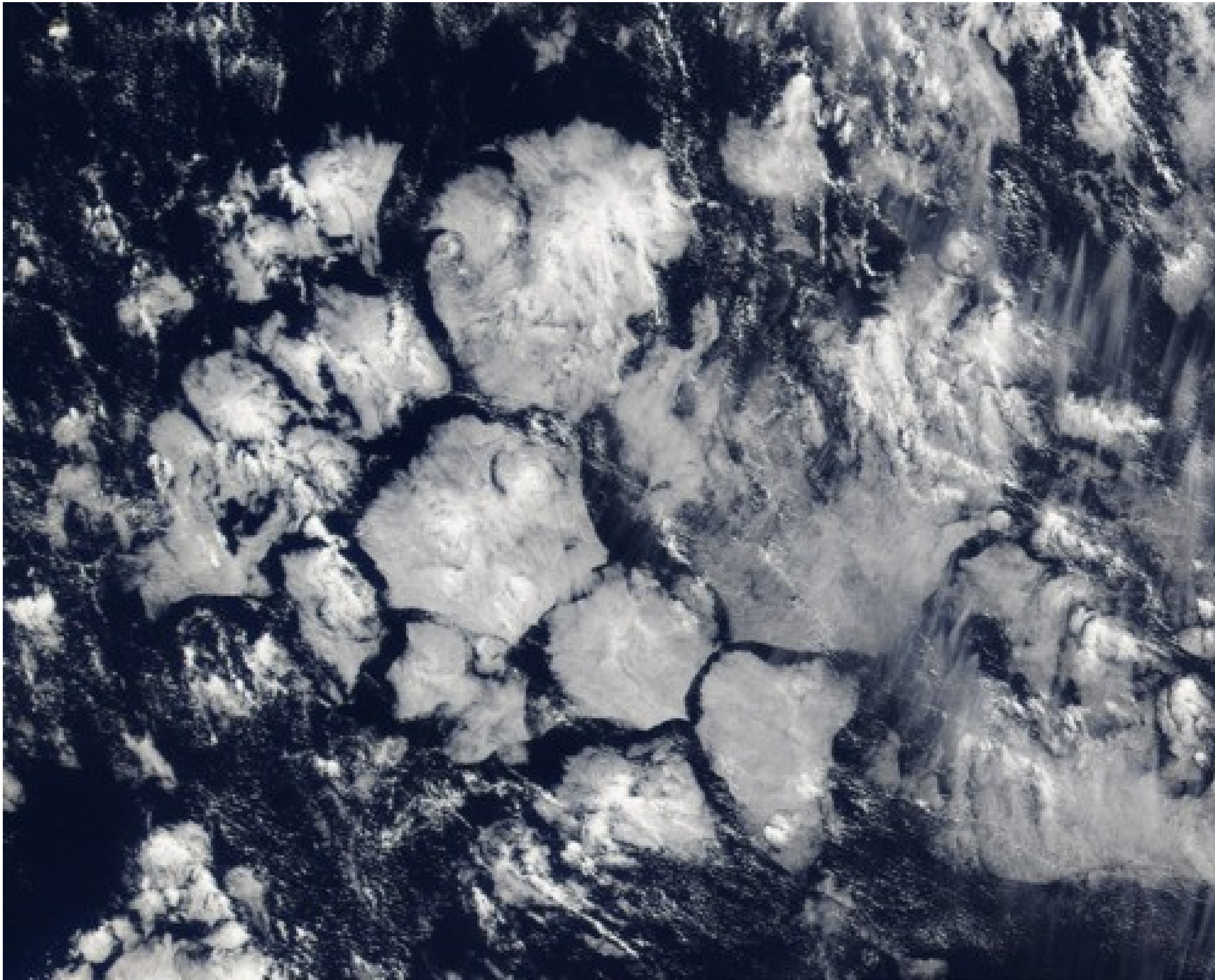

Can we simulate Rayleigh – Benard convection using numerical models ?

Yes, we can try!
But we will likely be underresolved, i.e. it is typically impossible to model all scales. That means we must trust our model to properly parametrize the unresolved scales.

Chaotic and organized convection in numerical simulations

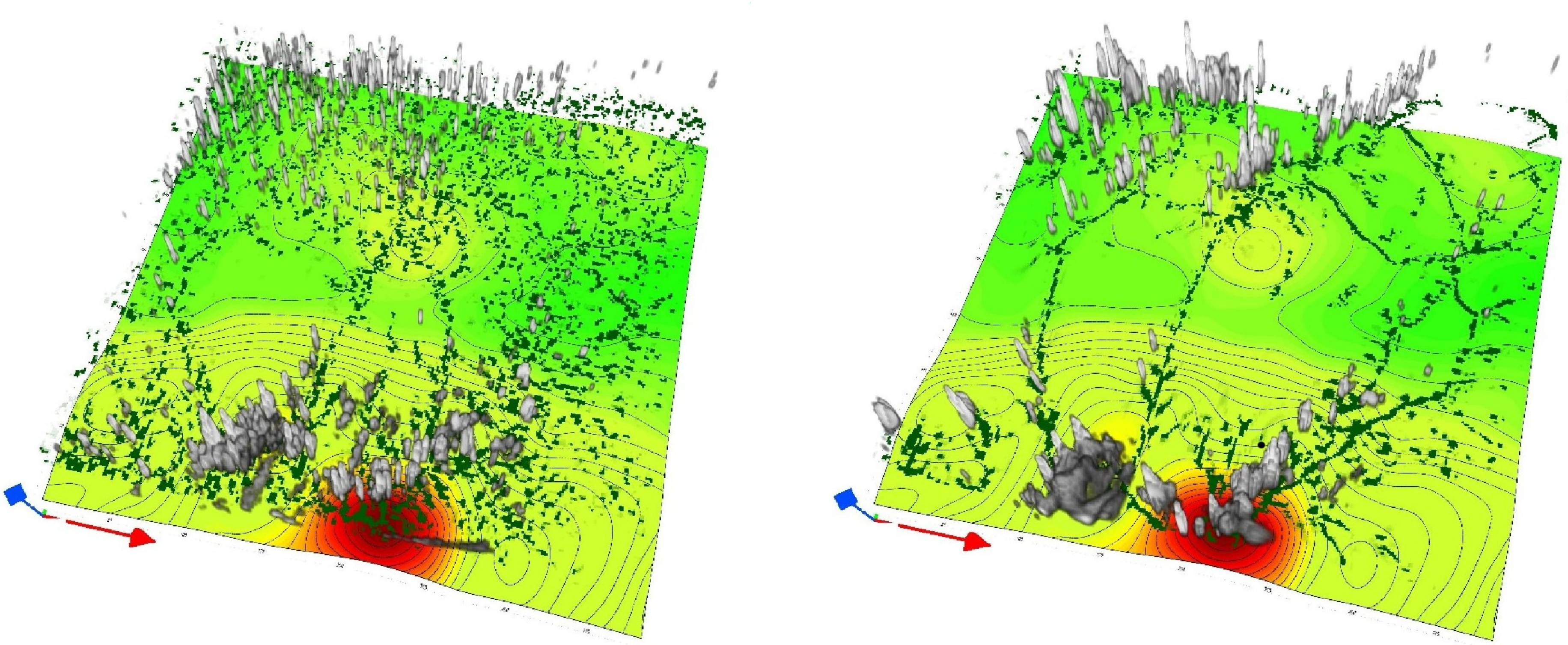

Structure of simulated convection over heated realistic terrain.

Vertical velocities after 6h of simulated time are shown within the PBL depth. Grey iso-surfaces represent clouds, and dark green patterns mark updrafts at boundary layer top. Isolines and other colors show the topography. ***The only difference between the two simulations is the effective viscosity of numerical advection.***

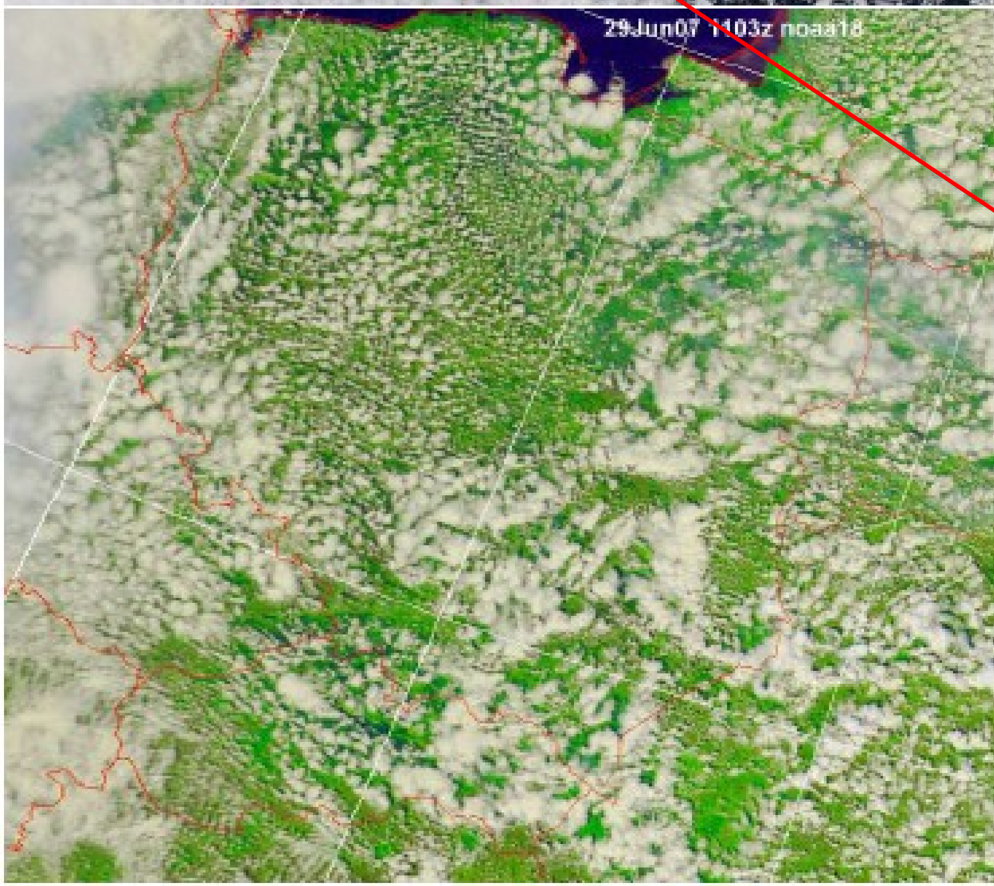

Cellular convection with characteristic size O(10 km)

Do we represent nature in this simulation?

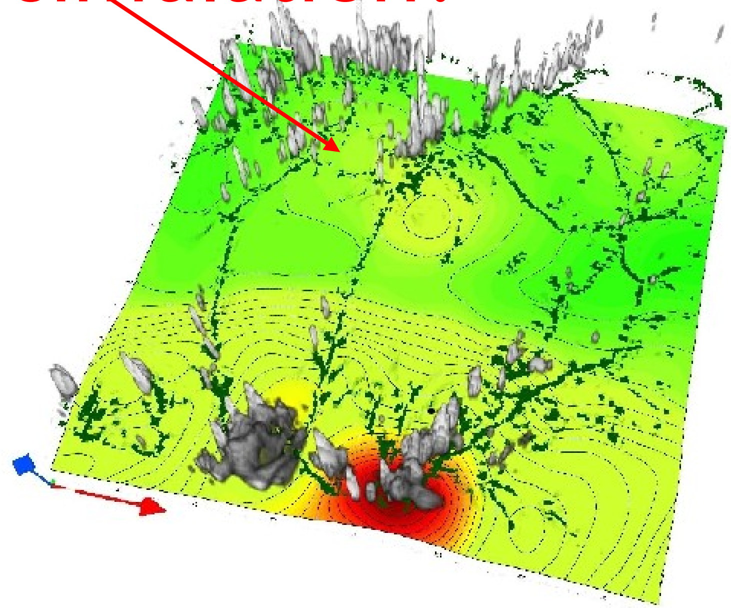

Rayleigh number in underresolved simulations

$$Ra = \frac{g\Delta\overline{\theta}h^3}{\overline{\theta}\nu\nu_\theta}$$

g – gravity acceleration
h – fluid layer thickness
ν – effective viscosity
ν_θ – effective diffusivity (=k)
Δθ /θ – pot. temperature, relative change over h

Ra measures relative magnitude of buoyancy and viscous forces

rigid/stress-free
lower/upper

Ra_c=1100.657

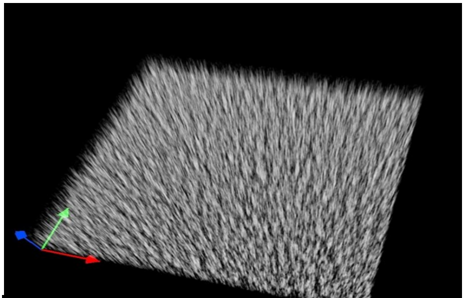

>> critical

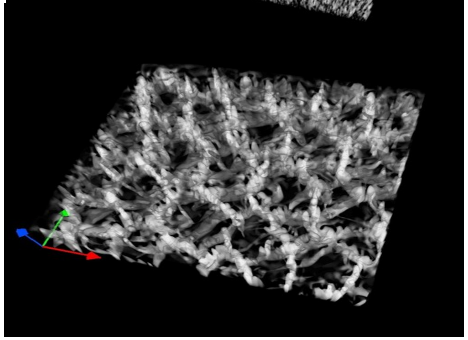

≈ critical

Convection over heated plane – effects of viscosity anisotropy
(separate effective viscosity attributed to the horizontal and vertical direction)

Piotrowski et al, “On numerical realizability of thermal convection”, JCP, Vol. 228, 2009

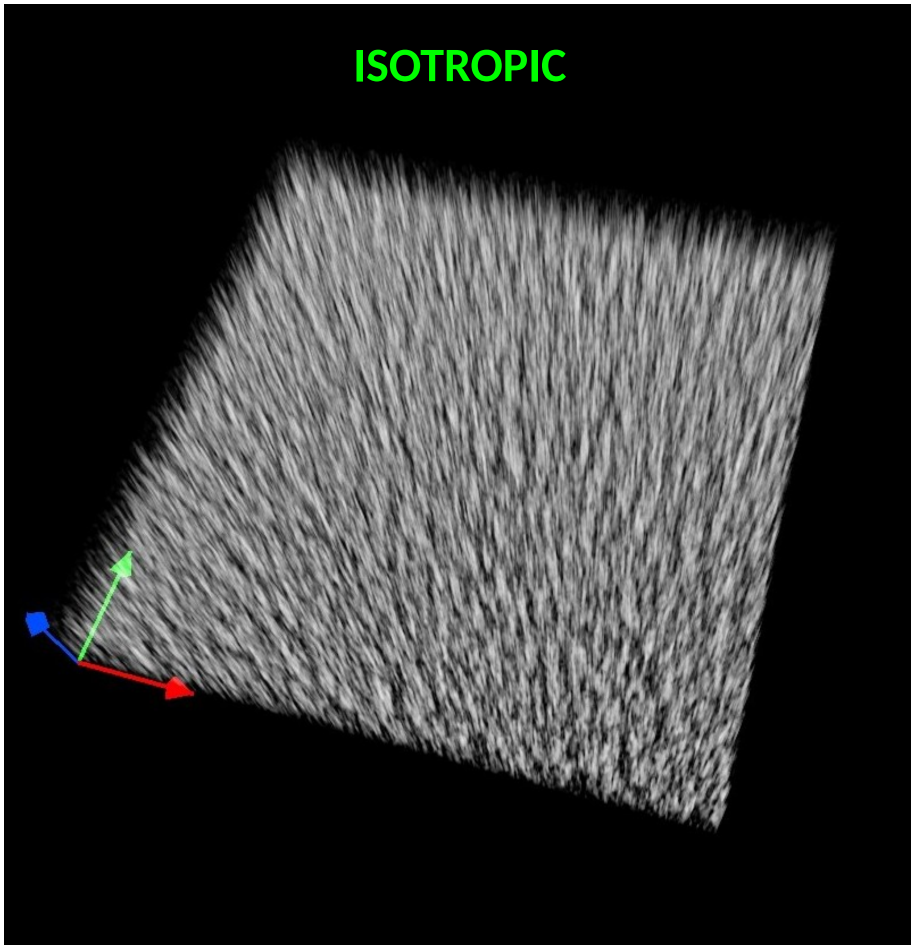

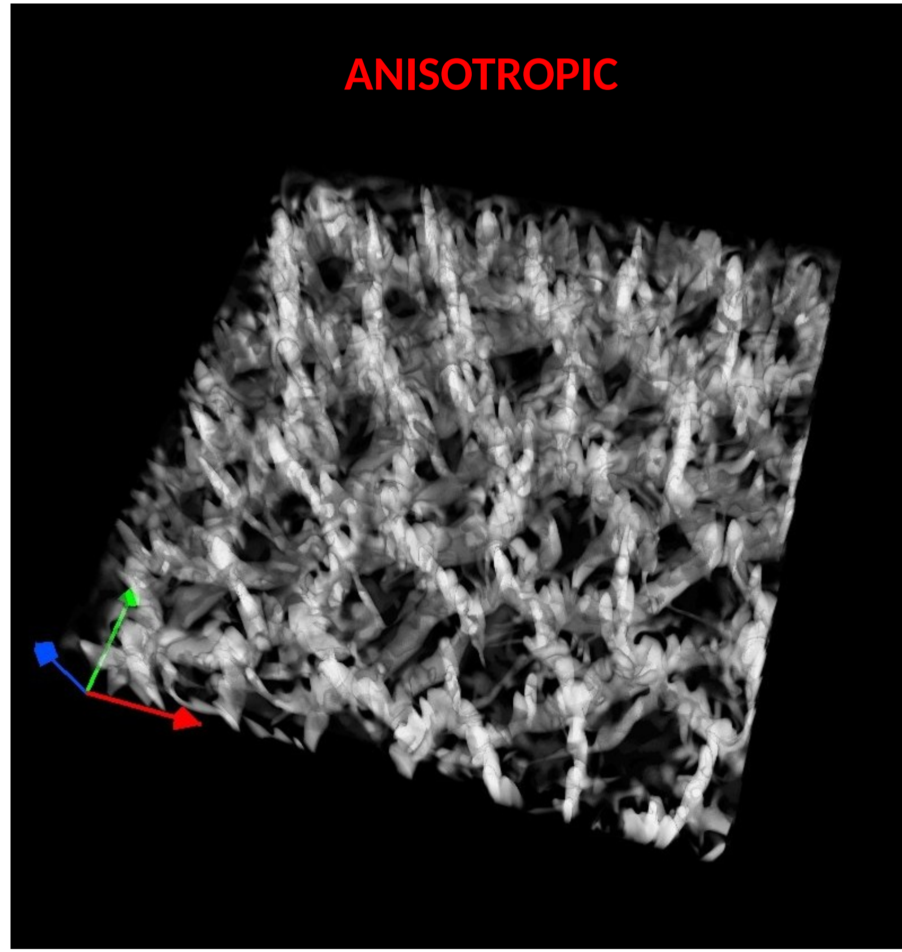

$n_v=k_v=2.5\ m^2s^{-1}$

$n_h=k_h=2.5\ m^2s^{-1}$

$r_n=r_k=1$

No mean wind, heatflux .2 Kms^{-1},

dx=dy=500 m, dz=50 m,

128x128x181 gridpoints

$n_v=k_v=2.5\ m^2s^{-1}$

$n_h=k_h=70\ m^2s^{-1}$

$r_n=r_k=3.6e\text{-}2$

Stability of the modes in function of wavenumber

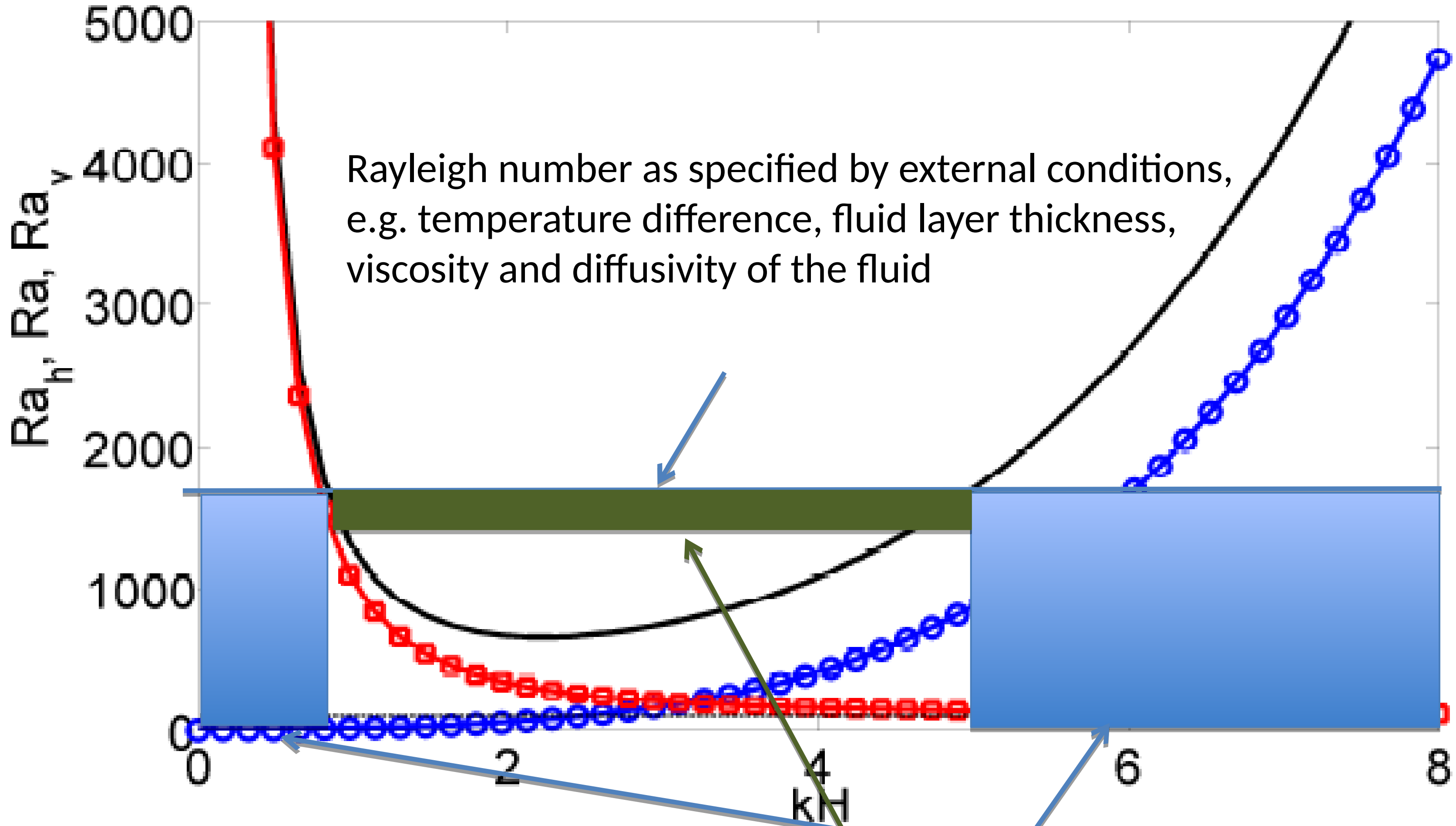

Classical result - stable modes are those for which constant Rayleigh number line lies below the black curve of marginal stability. Unstable modes which grow and we can observe are specified by green region.

In the dry atmosphere:

$h = 1000$ m
$\nu = 1.7 \times 10^{-5}$ m^2/s
$\nu_\theta = 1.9 \times 10^{-5}$ m^2/s
$\Delta\theta / \theta = O(10^{-3})$

$\longrightarrow$ **Ra ≈ O(10^{16})**

Thus, how to explain cellular convection ?

Modified definition (Jeffreys, 1928, Priestley 1962, Ray 1965, Sheu 1980)

$$Ra = \frac{g \Delta \overline{\theta} h^3}{\overline{\theta} K_m^2}$$

Km can be different in the horizontal and in the vertical.

Generalized governing equations for Rayleigh-Benard convection for anisotropic viscosity and Prandtl number anisotropy

Hadamard (entrywise) product

Momentum eq. $$\frac{\partial \mathbf{u}}{\partial t} = -\nabla\phi + g\alpha\theta\nabla z + \boldsymbol{\Delta}\circ\mathbf{u} \ ,$$

Temperature eq. $$\frac{\partial \theta}{\partial t} = \beta w + \kappa_h \partial_h^2\theta + \kappa_v \partial_z^2\theta \ ,$$

Continuity eq. $$\nabla\cdot\mathbf{u} = 0 \ ,$$

Vector laplacian $$\boldsymbol{\Delta} := (\widehat{\nu}_h\partial^2 + \triangle_0,\ \widehat{\nu}_h\partial^2 + \triangle_0,\ \widehat{\nu}_v\partial^2 + \triangle_0)$$

Scalar laplacian $$\triangle_0 := \nu_h\partial_h^2 + \nu_v\partial_z^2 \ , \quad \partial_h^2 := \partial_x^2 + \partial_y^2 \ ,$$

Linear theory extension – admitting full set of effective stress tensor entries

(separate effective viscosity attributed to horizontal and vertical direction AND each momentum equation)

$$\frac{\partial \mathbf{u}}{\partial t} = -\nabla\phi + g\alpha\theta\nabla z + \boldsymbol{\Delta}\circ\mathbf{u} \ ,$$

$$\frac{\partial \theta}{\partial t} = \beta w + \kappa_h \partial_h^2 \theta + \kappa_v \partial_z^2 \theta \ ,$$

$$\nabla\cdot\mathbf{u} = 0 \ ,$$

Prandtl number anisotropy – e.g. disparate approximations to momentum equations (full set of stress tensor entries)

$$\boldsymbol{\Delta} := \left(\widehat{\nu}_h\partial^2 + \triangle_0,\ \widehat{\nu}_h\partial^2 + \triangle_0,\ \widehat{\nu}_v\partial^2 + \triangle_0\right)$$

$$\triangle_0 := \nu_h\partial_h^2 + \nu_v\partial_z^2 \ , \quad \partial_h^2 := \partial_x^2 + \partial_y^2 \ ,$$

Anisotropic viscosity (coefficients at diagonal entries of stress tensor)

Applying operator of rotation to momentum equations:

$$\frac{\partial}{\partial t}(\nabla \times \mathbf{u}) = g\alpha \nabla \times \theta \nabla z + \boxed{\boxed{\triangle_0 \nabla \times \mathbf{u}}} + \boxed{\boxed{\Delta \nabla \times (\widehat{\nu} \circ \mathbf{u})}}$$

This term describes possible production of baroclinic vorticity

Taking rotation once again and considering the vertical component:

$$\frac{\partial}{\partial t}\partial^2 w = g\alpha \partial_h^2 \theta + \boxed{\boxed{\triangle_0 \partial^2 w}} + \boxed{\boxed{(\widehat{\nu}_v \partial_h^2 + \widehat{\nu}_h \partial_z^2)\partial^2 w}}$$

Equation set for vertical velocity and potential temperature becomes:

$$\left(\frac{d^2}{dz^2} - k^2\right)\left((\widehat{\nu}_h + \nu_v)\frac{d^2}{dz^2} - (\widehat{\nu}_v + \nu_h)\, k^2 - p\right)\hat{w} = g\alpha k^2 \hat{\theta}$$

$$\left(\kappa_v \frac{d^2}{dz^2} - \kappa_h k^2 - p\right)\hat{\theta} = -\beta \hat{w}\,.$$

Assuming solution in Fourier modes:

$$w = \hat{w}(z) \exp[i(k_x x + k_y y) + pt] \ ,$$
$$\theta = \hat{\theta}(z) \exp[i(k_x x + k_y y) + pt] \ ; \quad k^2 := k_x^2 + k_y^2 \ , \quad i := \sqrt{-1}$$

$$\left(\frac{d^2}{dz^2} - k^2\right)\left((\widehat{\nu}_h + \nu_v)\frac{d^2}{dz^2} - (\widehat{\nu}_v + \nu_h)\, k^2 - p\right)\hat{w} = g\alpha k^2 \hat{\theta}$$

$$\left(\kappa_v \frac{d^2}{dz^2} - \kappa_h k^2 - p\right)\hat{\theta} = -\beta \hat{w} \, .$$

Note that number of parameters is now effectively reduced.

$$\left(\frac{d^2}{dz^2} - k^2\right)\left(\nu_{veff}\frac{d^2}{dz^2} - \nu_{heff} k^2 - p\right)\left(\kappa_v \frac{d^2}{dz^2} - \kappa_h k^2 - p\right)\hat{w}$$
$$= -g\alpha k^2 \beta \hat{w} \, .$$

Linear theory
effects of viscosity anisotropy AND Prandtl number anisotropy

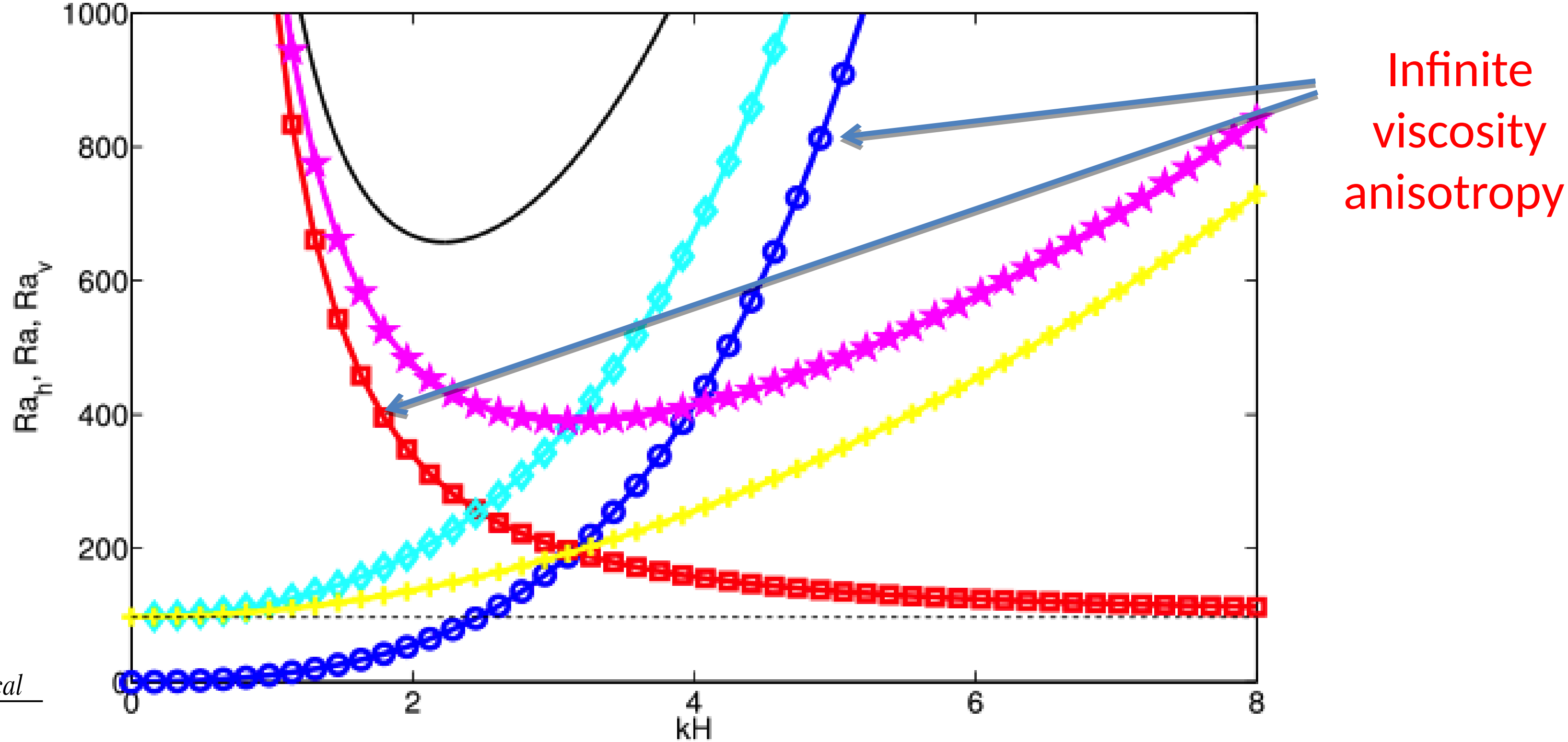

$$r_\upsilon = \frac{\upsilon_{vertical}}{\upsilon_{horizontal}}$$

Fig. 1. Asymptotic marginal stability relations for viscosities $\boxed{\nu_h = \nu_v}$ and thermal diffusivities $\boxed{\kappa_h = \kappa_v}$ (solid), viscosity anisotropy ratios $\boxed{r_{\nu,\kappa} = 0}$ (blue circles), $\boxed{r_{\nu,\kappa} = \infty}$ (red squares), $r_\nu = 0, r_\kappa = 1$ (cyan diamonds), $r_\nu = \infty, r_\kappa = 1$ (magenta stars), $r_\nu = \infty, r_\kappa = 0$ (yellow plus sign); here h and v denote respective values in the horizontal and the vertical. Corresponding Rayleigh numbers Ra are shown as functions of the non-dimensional horizontal wave number kH. For each curve the stability region lies beneath. The square, diamond and plus-sign asymptotics tend to the π^4 limit.

Linear theory
effects of viscosity anisotropy AND Prandtl number anisotropy

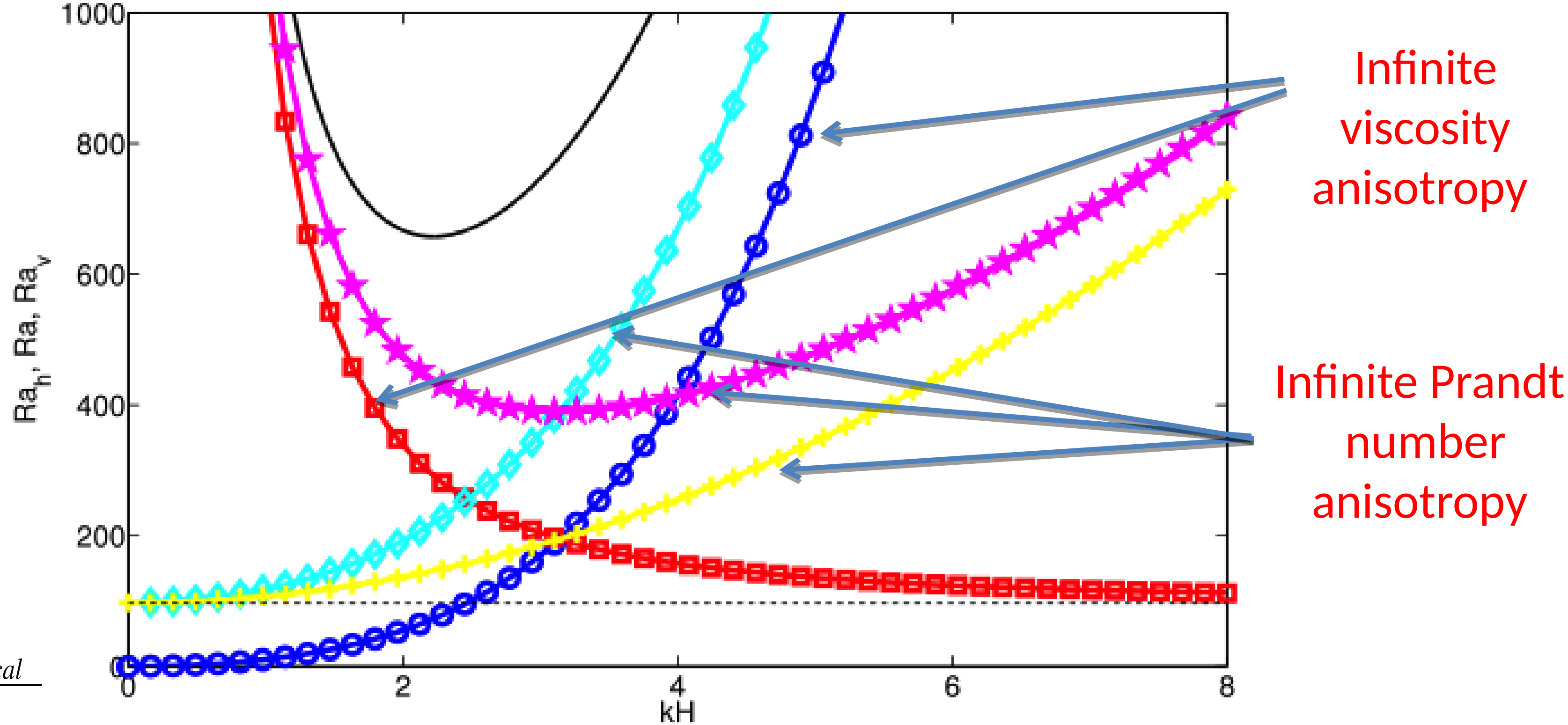

$$r_v = \frac{v_{vertical}}{v_{horizontal}}$$

Fig. 1. Asymptotic marginal stability relations for viscosities $\nu_h = \nu_v$ and thermal diffusivities $\kappa_h = \kappa_v$ (solid), viscosity anisotropy ratios $r_{\nu,\kappa} = 0$ (blue circles), $r_{\nu,\kappa} = \infty$ (red squares) $r_\nu = 0, r_\kappa = 1$ (cyan diamonds), $r_\nu = \infty, r_\kappa = 1$ (magenta stars), $r_\nu = \infty, r_\kappa = 0$ (yellow plus sign); here h and v denote respective values in the horizontal and the vertical. Corresponding Rayleigh numbers Ra are shown as functions of the non-dimensional horizontal wave number kH. For each curve the stability region lies beneath. The square, diamond and plus-sign asymptotics tend to the π^4 limit.

Analogy - Equation set for R-B convection in nematic liquid crystals:

STABILITY OF NEMATIC LIQUID CRYSTALS UNDER A TEMPERATURE GRADIENT. CALCULATIONS FOR PAA†

ATTILA AŞKAR‡
The Scientific and Technical Research Council T.B.T.A.K., Inşa
Turkey

$$\frac{\partial \mathbf{u}}{\partial t} = -\nabla\phi + g\alpha\theta\nabla z + \boldsymbol{\Delta}\circ\mathbf{u} \ ,$$
$$\frac{\partial \theta}{\partial t} = \beta w + \kappa_h\partial_h^2\theta + \kappa_v\partial_z^2\theta \ ,$$
$$\nabla\cdot\mathbf{u} = 0 \ ,$$

$$v_{1,1} + v_{3,3} = 0$$
$$t_{11,1} + t_{31,3} + \rho f_1 - \rho\left(\frac{\partial v_1}{\partial t} + v_1 v_{1,1} + v_3 v_{1,3}\right) = 0$$
$$t_{13,1} + t_{33,3} + \rho f_3 - \rho\left(\frac{\partial v_3}{\partial t} + v_1 v_{3,1} + v_3 v_{3,3}\right) = 0$$
$$m_{12,1} + m_{32,3} - (t_{13} - t_{31}) + \rho l_2 = 0$$
$$\frac{\partial T}{\partial t} + v_1 T_{,1} + v_3 T_{,3} + q_{1,1} + q_{3,3} = 0.$$

Similarly the constitutive relations read

$$t_{11} = -p + (a_{1111} - a_{1133})v_{1,1}$$
$$t_{33} = -p + (a_{3333} - a_{3311})v_{3,3}$$
$$t_{13} = a_{1331}v_{1,3} + a_{1313}v_{3,1} + (a_{1313} - a_{1331})\dot{\psi}_2$$
$$t_{31} = a_{3131}v_{1,3} + a_{3113}v_{3,1} + (a_{3113} - a_{3131})\dot{\psi}_2$$
$$m_{12} = B_{2121}\psi_{2,1}$$
$$m_{32} = B_{2323}\psi_{2,3}$$
$$q_1 = -(k_{11}T_{,1} + k_{13}T_{,3})$$
$$q_3 = -(k_{31}T_{,1} + k_{33}T_{,3})$$

These equation sets are very similar
in viscous tensor formulation,
when L.C. equations are linearized and
microrotation of crystals neglected.

Possible stress tensor realizations - two simple examples

Example 1: Prandtl number isotropy - anisotropic filtering of model equations

$n_v = k_v = x\ m^2 s^{-1}$

$n_h = k_h >> n_v = k_v$

$\hat{n}_v = \hat{n}_h = 0$

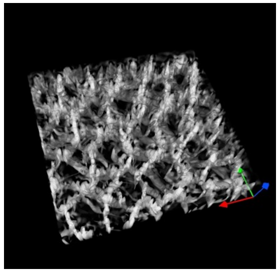

Example 2: Prandtl number anisotropy –anisotropic filtering of either momentum equations or temperature equation

$k_v = x\ m^2 s^{-1}$

$k_h >> k_v$

$n_v = n_h = x\ m^2 s^{-1}$

$\hat{n}_v = \hat{n}_h = 0$

… or in terms of extended linear theory

$k_v = x\ m^2 s^{-1}$

$k_h >> k_v$

$n_v = n_h = 0$

$\hat{n}_v = \hat{n}_h = x\ m^2 s^{-1}$

Numerical substantiation to follow ….

Possible stress tensor realizations - two simple examples

Example 1: Prandtl number isotropy - anisotropic filtering of model equations

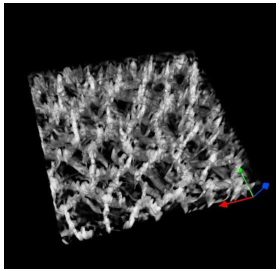

Horizontal viscosity and thermal diffusivity

much larger than

vertical viscosity and thermal diffusivity

Example 2: Prandtl number anisotropy –anisotropic filtering of either momentum equations or temperature equation

Viscosity is isotropic.

Horizontal thermal diffusivity

much larger than

vertical thermal diffusivity.

Numerical example to follow.

Example of numerical substantiation

Series of LES and ILES using the EULAG model

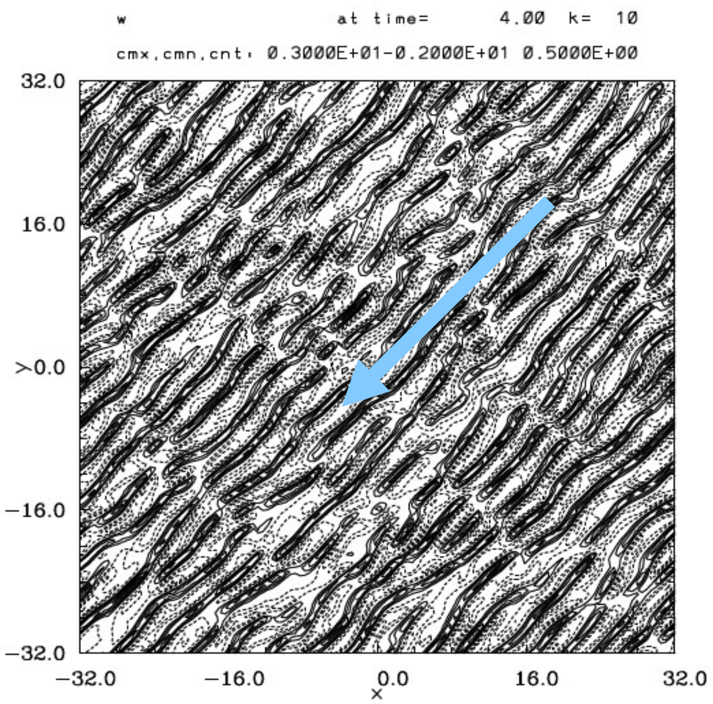

dz=50 m

dx=dy=500 m

V = [-10,-10] m/s

Heat flux
hfx≈200 W/m^2

Flat lower boundary, doubly periodic horizontal domain, Boussinesq option

Reference setup alludes to contemporary, mesoscale cloud-resolving NWP

Convective picture – reference ILES simulations, but with different filters (anisotropic viscosity)

Composite MPDATA: 1st order UPWIND every 4th dt

1-2-1 filter

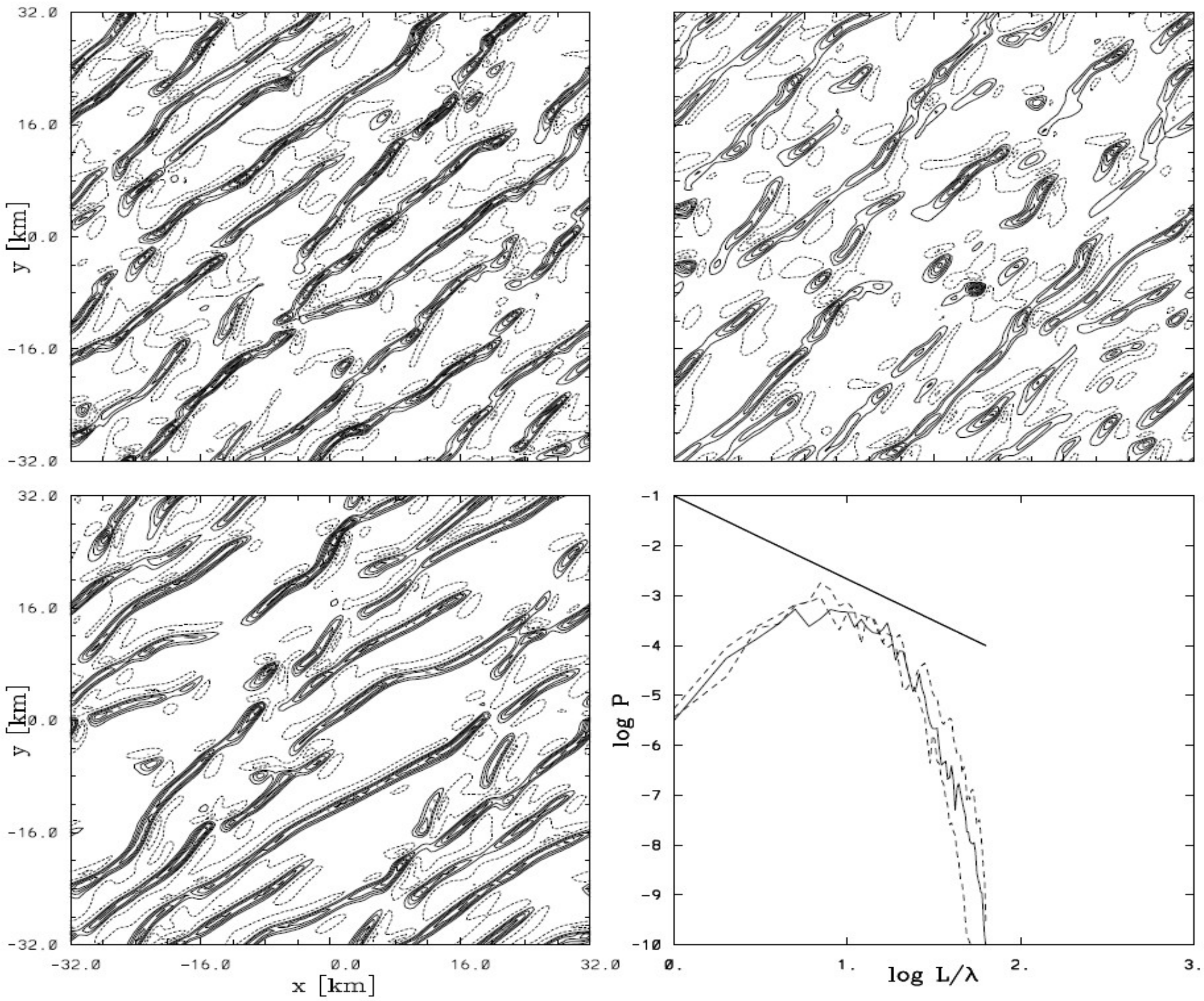

Explicit anisotropic viscosity

Diagonal 2D Spectra

Different filtering gives similar results

Example 1. refers to the “blue circle” asymptote

Example 2. refers to the “cyan diamond” asymptote

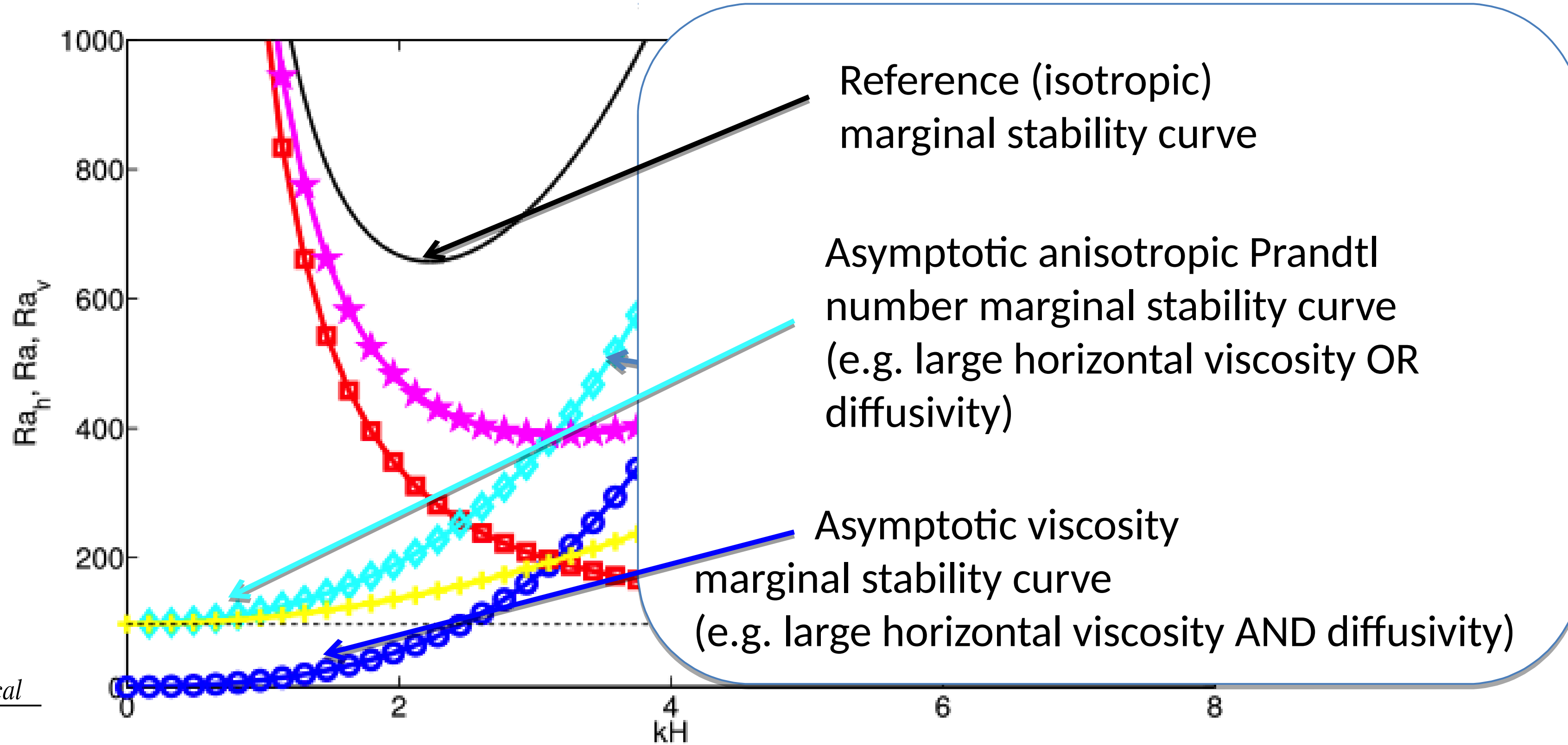

$$r_v = \frac{v_{vertical}}{v_{horizontal}}$$

Fig. 1. Asymptotic marginal stability relations for viscosities $\boxed{\nu_h = \nu_v}$ and thermal diffusivities $\boxed{\kappa_h = \kappa_v}$ (solid), viscosity anisotropy ratios $\boxed{r_{\nu,\kappa} = 0}$ (blue circles), $\boxed{r_{\nu,\kappa} = \infty}$ (red squares), $\boxed{r_\nu = 0, r_\kappa = 1}$ (cyan diamonds), $\boxed{r_\nu = \infty, r_\kappa = 1}$ (magenta stars), $\boxed{r_\nu = \infty, r_\kappa = 0}$ (yellow plus sign); here h and v denote respective values in the horizontal and the vertical. Corresponding Rayleigh numbers Ra are shown as functions of the non-dimensional horizontal wave number kH. For each curve the stability region lies beneath. The square, diamond and plus-sign asymptotics tend to the π^4 limit.

Convection over heated plane, heatflux .2 Kms^{-1}, dx=dy=125 m, dz = 50 m, 512x512x180 gridpoints

Reference Implicit LES solution after 4h of simulated time at 1/3 of the boundary layer depth.

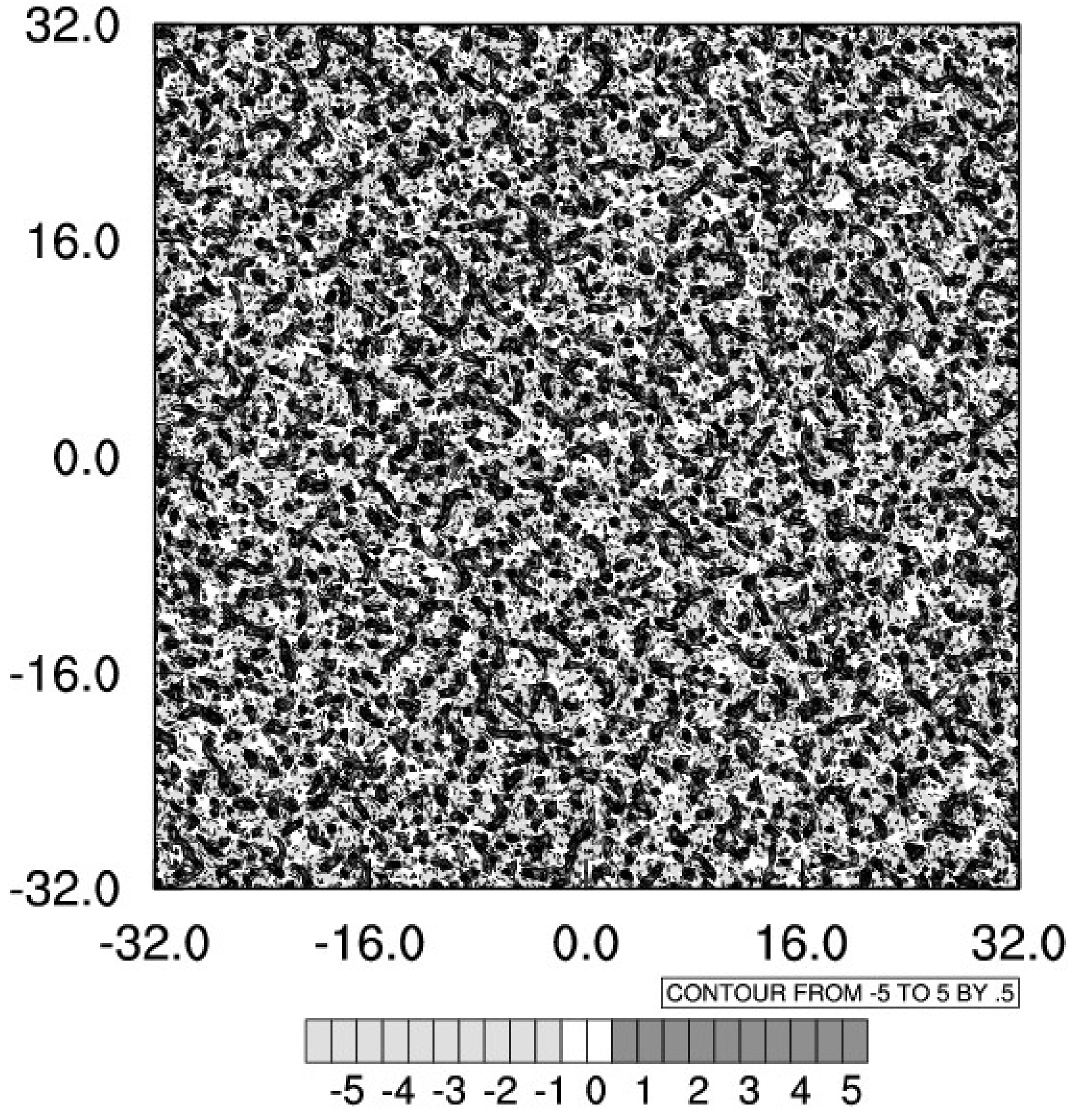

Convection over heated plane, heatflux .2 Kms^{-1}, dx=dy=125 m, dz = 50 m, 512x512x180 gridpoints

Illustration to example 1: anisotropic viscosity $r_n = r_k = 8e\text{-}2$.

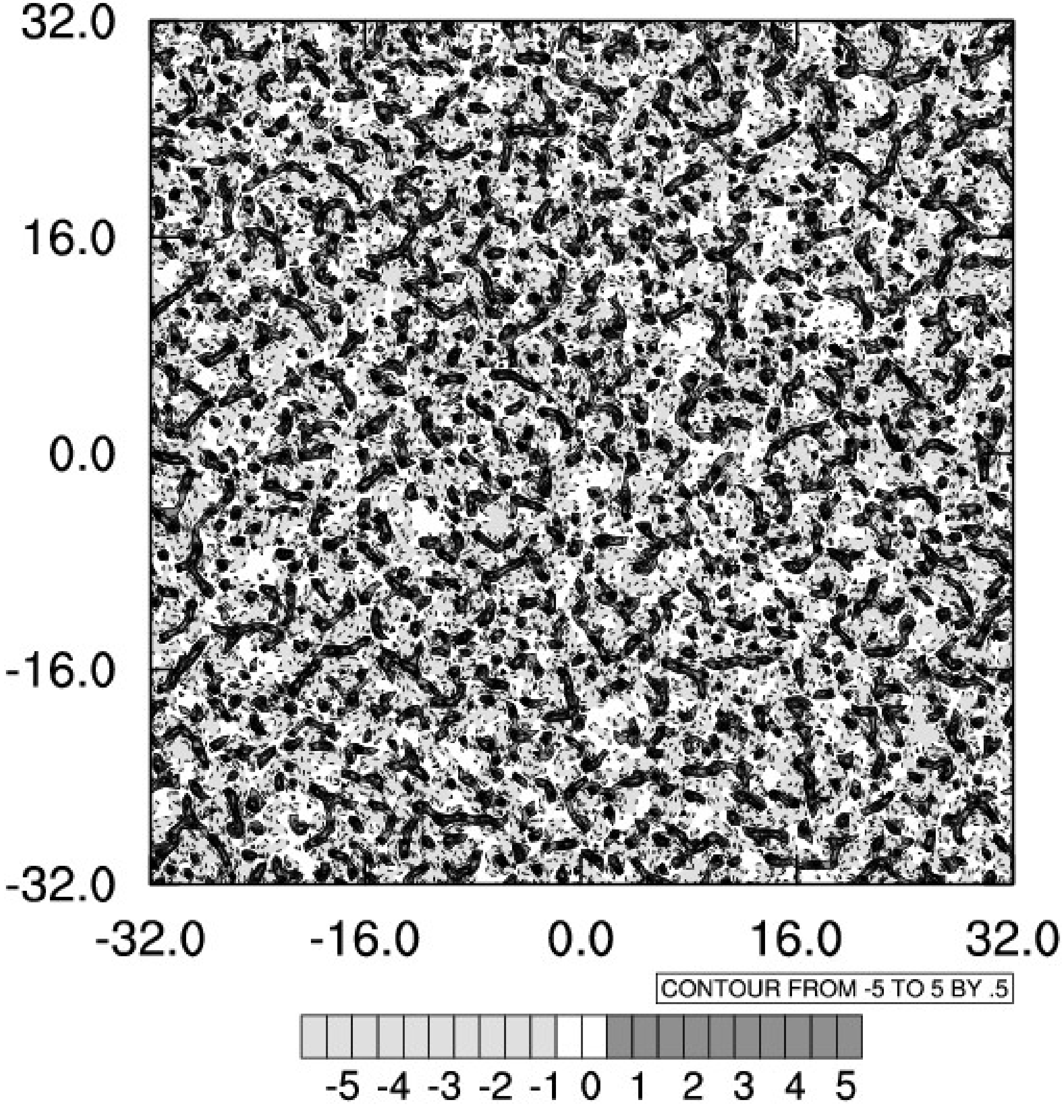

Convection over heated plane, heatflux .2 Kms^{-1}, dx=dy=125 m, dz = 50 m, 512x512x180 gridpoints

Illustration to example 2: Prandtl number anisotropy $Pr_v : Pr_h = 1 : 6e\text{-}3$. The same Rayleigh number as in example 1.

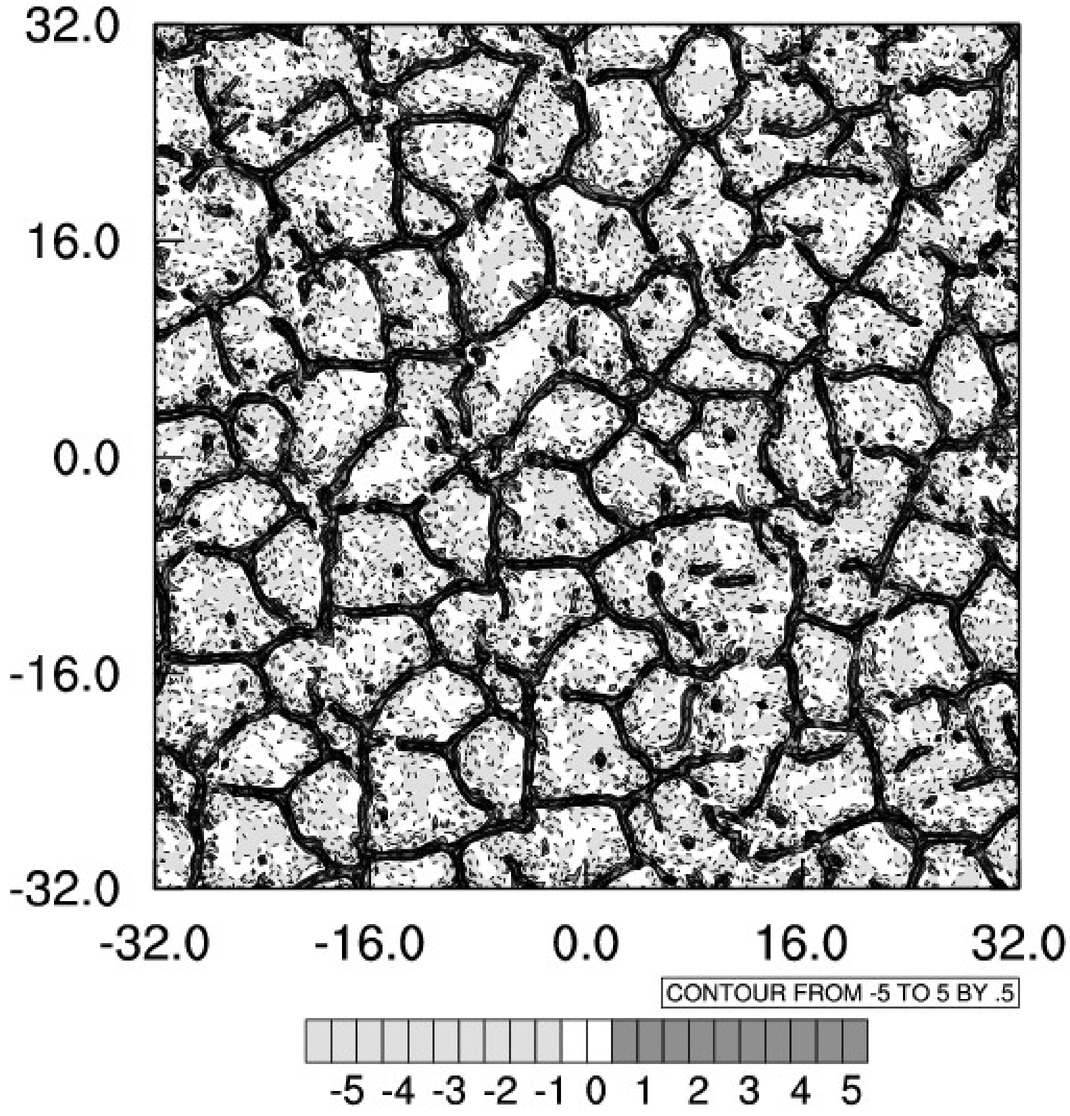

EULAG research model and COSMO-EULAG dynamical core of COSMO framework: numerical tools for studying convection in the greyzone.

- Non-oscillatory forward in time anelastic/compressible solvers of idealized and realistic weather scenarios, respectively

- Based on fully three-dimensional MPDATA advection suite + preconditioned Generalized Conjugate Residual implicit solvers,

- Independent of any numerical or physical diffusion for robustness, even for integrations over extremely steep slopes
- Akin to Finite Volume Module developed at ECMWF

Example of Alpine weather realization with COSMO-EULAG: effects of horizontal Smagorinsky diffusion (optional device of COSMO to prevent the model from a crash by horizontal shear instabilities).

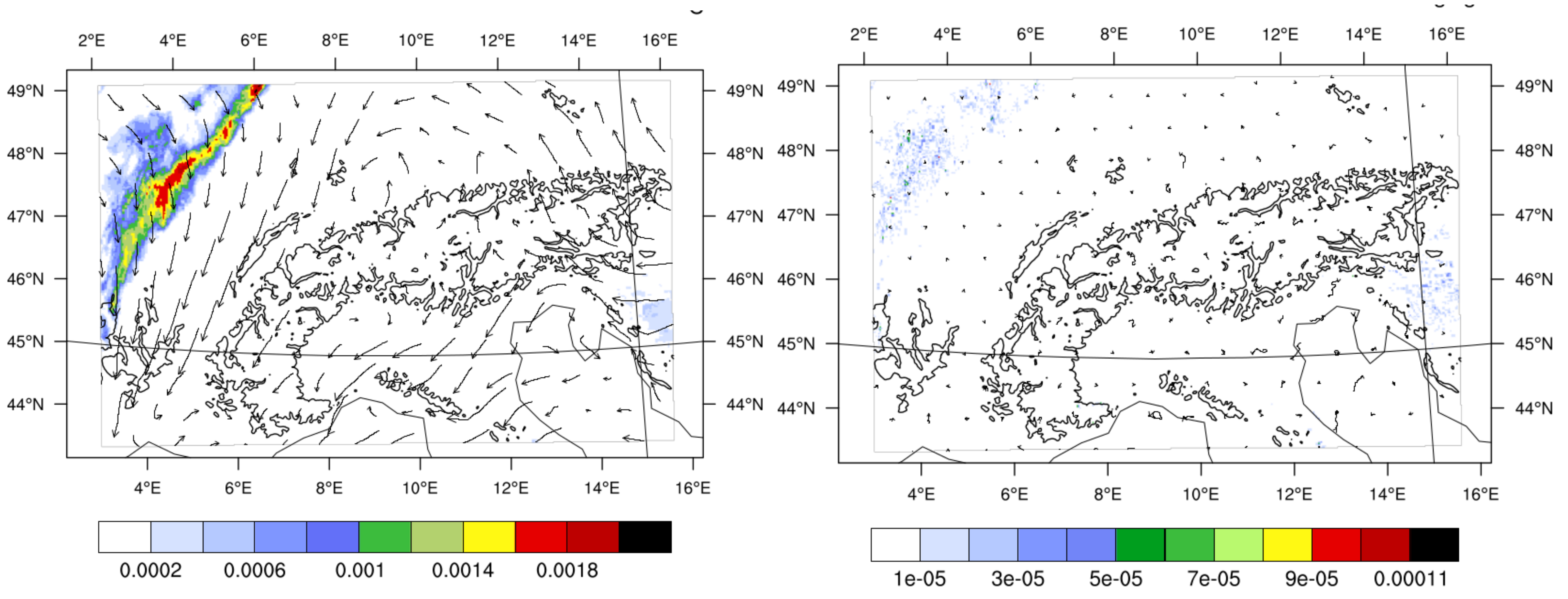

Conclusions

- Anisotropic viscosity and Prandtl number anisotropy can modify marginal stability and mode growth rates of realized R-B convection.
- Prandtl number anisotropy effects may alter convective picture at much higher Rayleigh number than anisotropic viscosity effects alone, due to a modification of the mode stability range and growth rate change.
- There may be an option to use the derived linear theory for tune a numerical model for specific task.